

# WAVECLIP: WAVELET TOKENIZATION FOR ADAPTIVE-RESOLUTION CLIP

Moshe Kimhi<sup>1,2\*</sup>

Erez Koifman<sup>1\*</sup>

Ehud Rivlin<sup>1</sup>

Eli Schwartz<sup>2†</sup>

Chaim Baskin<sup>3†</sup>

<sup>1</sup> Technion – Israel Institute of Technology    <sup>2</sup> IBM Research  
<sup>3</sup> Ben-Gurion University of the Negev

## ABSTRACT

We introduce WAVECLIP, a single, unified model for adaptive-resolution inference in CLIP, enabled by wavelet-based tokenization. WAVECLIP replaces standard patch embeddings with a multi-level wavelet decomposition, enabling the model to process images coarse-to-fine while naturally supporting multiple resolutions within the same model. At inference time, the model begins with low-resolution tokens and refines only when needed, using key-value caching and causal cross-level attention to reuse computation, effectively introducing to the model only new information when needed. We evaluate WAVECLIP in zero-shot classification, demonstrating that a simple confidence-based gating mechanism enables adaptive early exits. This allows users to dynamically choose a compute-accuracy trade-off using a single deployed model. Our approach requires only lightweight distillation from a frozen CLIP teacher and achieves competitive accuracy with significant computational savings.

**Index Terms**— CLIP, Wavelet, Inference, MultiModal

## 1. INTRODUCTION

Contrastive language-image pretraining (CLIP) enables strong zero-shot transfer with a frozen text tower and a Vision Transformer (ViT) image encoder [1, 2, 3]. However, its inference cost scales quadratically with the number of image tokens, leading to very high GFLOPs.

While much of the prior work on efficient CLIP reduces or redesigns the *vision tower* [4, 5, 6] or modifies the training objective [3, 7, 8], these approaches—though effective for accuracy or efficiency—typically require heavy pre-training on web-scale datasets (e.g., 2-5B examples). Moreover, each model is trained independently, yielding separate models for different scenarios. This makes it hard to dynamically adjust the trade-off at inference time and complicates deployment in systems that need adaptive behavior.

We introduce **WAVECLIP**, a training-light, drop-in alternative to patch tokenization that turns a multi-level discrete wavelet transform (DWT) into a *progressive, cacheable* inference schedule for CLIP. WAVECLIP processes coarse tokens first (LL band) and exits early when confident; otherwise, it *appends* level-wise

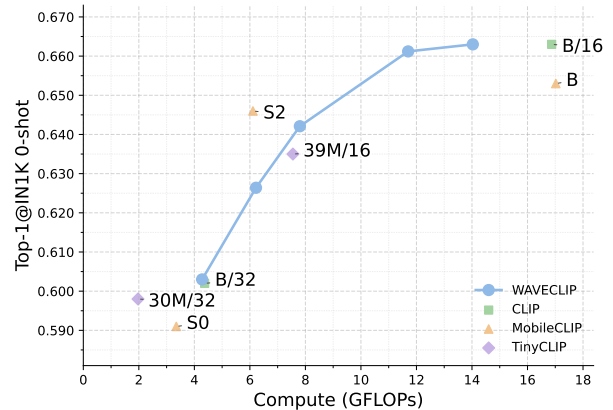


**Fig. 1. Accuracy-compute frontier on ImageNet-1k (zero-shot).** WAVECLIP spans a smooth trade-off curve by adjusting threshold at inference, while prior methods appear as fixed points—each requiring a separate model for a single compute budget.

detail tokens (LH/HL/HH). A block-causal cross-level attention mask allows tokens at level  $\ell$  to attend to tokens from levels  $\leq \ell$ , so key/value states are reused and prior computation is never repeated. A short distillation from a frozen CLIP teacher preserves zero-shot alignment, avoiding full image-text pretraining.

**Our contributions:** (i) A wavelet tokenizer + cross-level attention mask that enables early exits with KV reuse in CLIP, no ViT/text-tower changes. (ii) A light distillation procedure that maintains zero-shot alignment. (iii) Accuracy/compute trade-offs via simple confidence gating, that is controllable at inference time.

## 2. RELATED WORK

In CLIP-specific efficiency, most prior work shrinks or redesigns the *vision tower* itself: TinyCLIP distills large CLIP models into compact students [4]; MobileCLIP trains lightweight backbones with multimodal reinforcement [5]; and MobileCLIP2 further strengthens distillation/captioning for improved zero-shot at similar runtimes [6]. These approaches trade parameters and capacity for speed. *In contrast, we keep the standard CLIP ViT and text tower intact* [9, 1, 2, 3] and target *how much* visual evidence is processed per image.

\*Equal contribution

†Equal supervision

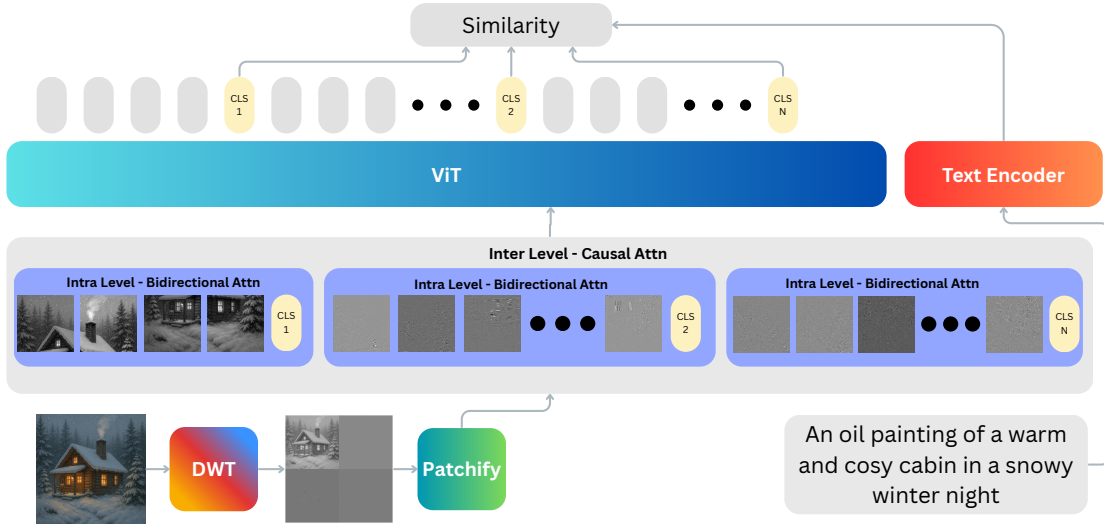


**Fig. 2. WAVECLIP overview.** A discrete wavelet transform (DWT) decomposes the image and, after patchify, yields multiscale token groups. Inference proceeds coarse-to-fine in a single Transformer: each group uses bidirectional attention internally, while a causal cross-level mask lets later groups attend to earlier tokens only.

Early-exit methods dynamically adjust compute based on input difficulty, by forecasting predictions from earlier layers of the model [10, 11]; this differs from our approach, as deciding to process fewer (coarser) tokens directly reduces GFLOPs when the model architecture stays intact, enabling robust deployment and KV-cache reuse.

*Multiscale tokenization.* Wavelet decompositions provide a principled, dyadic multiresolution representation [12, 13] and have recently been explored as drop-in tokenizers for ViTs [14]. We leverage this structure not only to replace patchify, but to enable *progressive, cacheable* inference: start from the coarse LL band and *only* add LH/HL/HH detail when the gate deems it necessary. A block-causal cross-level attention mask and key-value (KV) caching let finer levels reuse keys/values from coarser levels, avoiding recomputation while preserving the standard CLIP architecture.

### 3. METHOD

Given an image  $x \in \mathbb{R}^{H \times W \times 3}$  and a ViT image encoder with  $B$  transformer blocks, a standard patch embedder with patch size  $P$  yields  $N = \frac{HW}{P^2}$  spatial tokens (plus a [CLS] token). Self-attention incurs  $O(N^2d)$  cost per block, so reducing  $N$  directly lowers GFLOPs. In CLIP-style zero-shot inference, an image embedding  $v \in \mathbb{R}^d$  is compared to a bank of text embeddings  $\{t_m\}_{m=1}^M$  via cosine similarity.

#### 3.1. Wavelet decomposition as structured tokenization

Instead of patchify, we first convert  $x$  from RGB to YCbCr and apply an  $L$ -level 2D discrete wavelet transform (DWT)

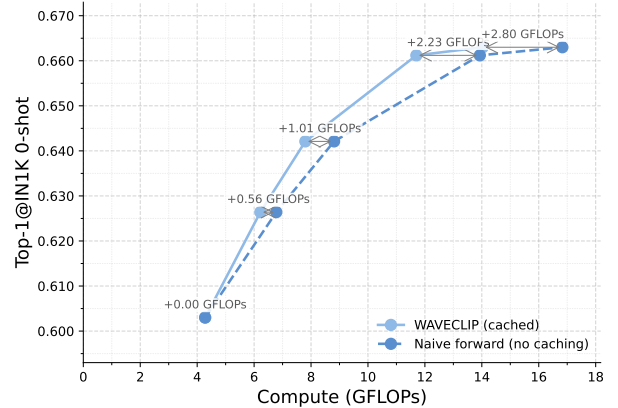


**Fig. 3.** Comparing the computational cost of using KV cache vs no KV cache reuse.

*independently to each channel*, producing channel-wise subbands

$$\{(\text{LL}^{(\ell,c)}, \text{LH}^{(\ell,c)}, \text{HL}^{(\ell,c)}, \text{HH}^{(\ell,c)})\}_{\ell=1, c \in \{Y, \text{Cb}, \text{Cr}\}},$$

with dyadic scaling [12, 13];  $\text{LL}^{(L,c)}$  is the coarsest approximation for channel  $c$ , while LH/HL/HH add band-pass detail at progressively finer scales. We tokenize each subband by non-overlapping  $P \times P$  patches and then *merge* tokens from all channels, ordering them coarse-to-fine across levels (and channels), following evidence that wavelet tokenizers can replace patchify in ViTs [14]. Unlike [14], which concatenates DWT subbands along the channel dimension to preserve the spatial grid and thus keep the token count  $N$ , we explicitly *reduce* the

number of tokens by processing coarse (LL) tokens first and appending LH/HL/HH detail only when needed, directly lowering the quadratic attention term and GFLOPs. Denote the cumulative token set after  $\ell$  refinement steps by

$$\begin{aligned}\mathcal{X}^{[0]} &= \text{patchify}(\text{LL}^{(L)}) \\ \mathcal{X}^{[\ell]} &= \mathcal{X}^{[s-1]} \cup \text{patchify}(\mathcal{D}^{(L-s+1)}), \ell=1, \dots, L\end{aligned}$$

where  $\mathcal{D}^{(\ell)} = \{\text{LH}^{(\ell)}, \text{HL}^{(\ell)}, \text{HH}^{(\ell)}\}$ . Thus  $\mathcal{X}^{[L]}$  equals the full-resolution token set. This design lets us begin with very few coarse tokens and add detail only when needed, directly controlling  $N$ .

### Token counts:

At level  $\ell$ , spatial size  $\frac{H}{2^\ell} \times \frac{W}{2^\ell}$ , yielding  $\frac{HW}{P^2 4^\ell}$  tokens. Hence

$$N_{\text{coarse}} = \frac{HW}{P^2 4^L} + 1, \quad N^{[s]} = \frac{HW}{P^2} \left( \frac{1}{4^L} + \sum_{\ell=L-s+1}^L \frac{3}{4^\ell} \right) + s,$$

where  $+s$  accounts for [CLS].

We train the model with the new DWT tokenizer and new [CLS] tokens to align with the original CLIP embedding space using a pretrained CLIP teacher. Given a student embedding  $v^{[\ell]}$  for the  $\ell$ 's [CLS] token, and teacher embedding  $v_T$ , we minimize the cosine distance:

$$\mathcal{L}_{\text{distill}} = \sum_{\ell=1}^L 1 - \frac{\langle v^{[\ell]}, v_T \rangle}{\|v^{[\ell]}\| \|v_T\|}$$

### 3.2. Causal cross-level attention with KV reuse

Let  $f_\theta$  denote the ViT image encoder. We enforce *level causality* via a block-lower-triangular (by level) attention mask: tokens introduced at level  $\ell$  may attend to tokens from level  $\leq \ell$ , but not vice versa. Formally, with cached key/value states  $\mathcal{KV}^{[\ell-1]}$  from previous levels,

$$v^{[s]} = f_\theta(\mathcal{X}^{[s]}; \mathcal{KV}^{[s-1]}, M_{\leq s}), \quad (1)$$

where  $M_{\leq s}$  is the cross-level causal mask. This allows *incremental* computation: upgrading from  $s-1$  to  $s$  reuses  $\mathcal{KV}^{[s-1]}$  and primarily pays for interactions involving the new tokens, avoiding recomputation on earlier tokens.

Fig. 2 illustrates the tokenization 3.1 and causality 3.2. While Fig. 3 shows the additional compute requires for naively forwarding all image tokens again, vs our KV cache reuse, advocating for the benefits of using Wavelet for tokenization.

### 3.3. Progressive inference for zero-shot classification

At level  $\ell$ , we score classes with temperature-scaled cosine similarity

$$s_m^{[\ell]} = \langle \text{norm}(v^{[\ell]}), \text{norm}(t_m) \rangle, \quad m=1, \dots, M, \quad (2)$$

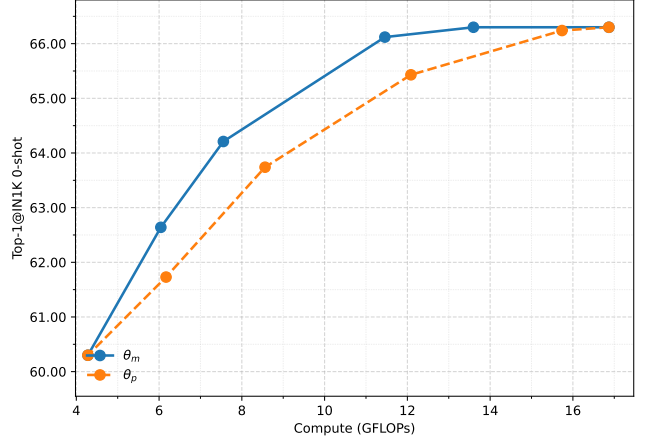


Fig. 4. Margin ( $\theta_m$ ) vs. confidence ( $\theta_p$ ) gating.

Similar to [15, 16] we apply a confidence gate to decide whether to *exit* or to *refine* (i.e., append the next finer level). We use a margin gate,

$$s_{(1)}^{[\ell]} - s_{(2)}^{[\ell]} \geq \theta_m \Rightarrow \text{exit at level } \ell, \quad (3)$$

where  $s_{(1)}^{[\ell]}$  and  $s_{(2)}^{[\ell]}$  are the top-1 and top-2 scores. Margin gating is empirically more stable across datasets than a fixed top-1 probability threshold, reducing the need for per-dataset calibration. When the condition is not met, we move to level  $\ell+1$  (if  $\ell \leq L$ ), reuse  $\mathcal{KV}$ , and evaluate again. This yields a single-pass behavior for easy images and coarse-to-fine refinement for hard images.

We compare our strategy to simple thresholding the max prob.  $s_{(1)}^{[\ell]} > \theta_p$ . while simple, score thresholding must be *carefully selected on a calibration set*, and, as shown in Fig. 4, empirically harder to separate between samples that requires only coarse information.

### 3.4. Complexity and control

Because attention scales quadratically in token count, operating at smaller  $N^{[s]}$  substantially reduces GFLOPs. The threshold  $\theta_m$  acts as an *inference-time knob* that trades accuracy for compute and can be adapted to constraints such as device budgets or low-battery modes, without modifying the trained model. We choose  $\theta_m$  to be relative to the number of classes in the dataset. e.g.  $\theta_m = p \cdot N$  where  $N$  is the number of classes in the dataset.

## 4. EXPERIMENTS

**Model** The teacher is a frozen CLIP ViT-B/16. WAVECLIP replaces *patchify* with an  $L=2$ -level discrete wavelet tokenizer while keeping the ViT image tower and the text tower unchanged.

**Progressive inference** At test time, tokens are processed coarse  $\rightarrow$  fine using a block-causal cross-level attention mask. Key-value states from coarser levels are cached and reused when adding finer tokens, so earlier computation is not repeated.

**Table 1.** Token counts for  $P=16$ ,  $H=W=224$ .  $L$  is the number of DWT levels;  $\ell$  is the number of refinement levels used. Counts include [CLS]; rows with  $\ell>0$  also include one level marker per level.

Levels $L$	$\ell=1$	$\ell=2$	$\ell=3$	$\ell=4$
$L=1$	197	–	–	–
$L=2$	50	198	–	–
$L=3$	13	51	199	–
$L=4$	4	14	52	200

---

**Algorithm 1** WAVECLIP Progressive Inference

---

**Require:** image  $x$ , Visual Encoder  $f_\theta$  text embeddings  $\{t_m\}$ , threshold  $\theta_m$

- 1: Compute  $L$ -level DWT:  $LL^{(L)}$ ,  $\mathcal{D}^{(\ell)}$  for  $\ell=1,\dots,L$
- 2:  $s \leftarrow 0$ ,  $\mathcal{X}^{[0]} \leftarrow \text{patchify}(LL^{(L)})$ ,  $KV \leftarrow \emptyset$
- 3: **repeat**
- 4:   Compute visual representation  $v^{[s]}$  (Eq. 1)
- 5:   Compute scores  $s^{[s]}$  (Eq. 2)
- 6:   **if** Sufficient (Using Eq. 3) **then**
- 7:     **return** prediction at level  $\ell$
- 8:   **else**
- 9:      $\ell \leftarrow \ell + 1$
- 10:     $\mathcal{X}^{[\ell]} \leftarrow \mathcal{X}^{[\ell-1]} \cup \text{patchify}(\mathcal{D}^{(L-\ell+1)})$
- 11:   **end if**
- 12: **until**  $\ell = L$
- 13: **return** prediction with all image tokens at level  $L$

---

**Evaluation** We report zero-shot ImageNet-1k validation accuracy (Top-1) using standard CLIP prompts. Metrics include per-image GFLOPs (image tower) and average tokens processed. Figures 1 and 3, and Table 2, summarize the results, where for WAVECLIP, **low**, **mid** and **high** refer to the margin threshold (yielding 26%, 57% and 74% of samples require all tokens).

All comparisons use  $224 \times 224$  input resolution. GFLOPs are reported for the *image encoder only*; text embeddings are computed once per prompt set. For WAVECLIP “Tokens” column reports expected visual tokens. Baseline models were trained on datasets of up to  $\approx 400$ M samples; for MobileCLIP and MobileCLIP2 we report accuracies from their longer training regimen (up to  $\approx 1$ B seen samples). All accuracies are ImageNet-1k zero-shot with standard CLIP prompts.

#### 4.1. Accuracy vs Compute Trade-off

Fig. 1 shows that WAVECLIP forms a smooth accuracy vs GFLOPs frontier using a *single* deployed model with different gating thresholds.

**Operating points.** Using margin threshold  $\theta_m$ , it is possible to change the operating point for a deployed model. For example, with  $p = 0.03$ , at **11.7 GFLOPs** WAVECLIP attains **66.12%**, yielding a  $\sim 30.6\%$  compute reduction. At the high-accuracy end, where  $p = 0.5$  WAVECLIP-H matches ViT-B/16 accu-

**Table 2.** Number of tokens, GFLOPs and Zero-shot ImageNet-1k vs prior CLIP-efficiency methods

Method	Res	Tokens	GFLOPs	IN1k
TinyCLIP (ViT-8M/16)	224	197	1.59	41.1
Open CLIP (ViT-B/32)	224	50	4.37	62.9
<b>WAVECLIP-low</b> (ViT-B/16)	224	71.93	6.22	62.6
TinyCLIP (ViT-39M/16)	224	197	7.55	63.5
MobileCLIP-S2 (Conv)	224	–	7.11	64.6
<b>WAVECLIP-mid</b> (ViT-B/16)	224	89	7.8	64.2
CLIP ViT-B/16	224	197	16.87	66.3
MobileCLIP-B (RegNetY-B)	224	–	17.02	65.3
MobileCLIP2 (RegNetY-B)	224	–	17.02	66.0
<b>WAVECLIP-high</b> (ViT-B/16)	224	160	14.03	66.3

racy (66.3%) at 14.03 GFLOPs, a  $\sim 16.8\%$  reduction over the baseline’s 16.87 GFLOPs. Tab. 2 reports representative points, including the average tokens used by WAVECLIP at each operating regime. Unlike alternatives that train separate networks for different budgets, WAVECLIP exposes a tunable accuracy-compute knob via early exits, simplifying deployment under dynamic constraints.

#### 4.2. Effect of KV Caching

Fig. 3 isolates KV reuse: we compare *cached* progressive inference (our default) to a *naive forward* that re-encodes all tokens at each refinement. For the same accuracy points, naive forward incurs an additional +0.56, +1.01, +2.23, and +2.80 GFLOPs as resolution increases (up to  $\sim 20\%$  overhead at the deepest point), whereas caching amortizes earlier computation. This confirms that cross-level causality plus KV reuse is critical for practical coarse-to-fine inference.

## 5. CONCLUSION

We presented WAVECLIP, an adaptive-resolution alternative to CLIP that (i) replaces patchify with a multi-level wavelet tokenizer, (ii) using a block-causal cross-level attention mask, and (iii) reuses computation via KV caching. This design enables coarse $\rightarrow$ fine inference in a *single* ViT image tower, exposing a simple trade of accuracy vs. compute at test time without retraining multiple models or altering the text tower. WAVECLIP attains near-baseline zero-shot accuracy on ImageNet-1k while reducing image-tower GFLOPs at matched accuracy (up to  $\sim 30\%$ ), yielding practical compute savings and a deployment-friendly model for resource-constrained scenarios as the compute–performance trade-off can be dynamically adjusted at inference. For future work, WAVECLIP could be particularly beneficial for high-resolution images, where computational demands increase substantially. Higher-resolution inputs would allow the use of additional decomposition levels in the wavelet tokenizer, enabling exponentially higher compute savings by utilizing the early exit strategy presented.

## 6. REFERENCES

- [1] Alec Radford, Jong Wook Kim, Chris Hallacy, Aditya Ramesh, Gabriel Goh, Sandhini Agarwal, Girish Sastry, Amanda Askell, Pamela Mishkin, Jack Clark, Gretchen Krueger, and Ilya Sutskever, “Learning transferable visual models from natural language supervision,” 2021.
- [2] Mehdi Cherti, Romain Beaumont, Ross Wightman, Mitchell Wortsman, Gabriel Ilharco, Cade Gordon, Christoph Schuhmann, Ludwig Schmidt, and Jenia Jitsev, “Reproducible scaling laws for contrastive language-image learning,” in *Proceedings of the IEEE/CVF Conference on Computer Vision and Pattern Recognition*, 2023, pp. 2818–2829.
- [3] Xiaohua Zhai, Basil Mustafa, Alexander Kolesnikov, and Lucas Beyer, “Sigmoid loss for language image pre-training,” 2023.
- [4] Kan Wu, Houwen Peng, Zhenghong Zhou, Bin Xiao, Mengchen Liu, Lu Yuan, Hong Xuan, Michael Valenzuela, Xi (Stephen) Chen, Xinggang Wang, Hongyang Chao, and Han Hu, “Tinyclip: Clip distillation via affinity mimicking and weight inheritance,” in *Proceedings of the IEEE/CVF International Conference on Computer Vision (ICCV)*, October 2023, pp. 21970–21980.
- [5] Pavan Kumar Anasosalu Vasu, Hadi Pouransari, Fartash Faghri, Raviteja Vemulapalli, and Oncel Tuzel, “Mobileclip: Fast image-text models through multi-modal reinforced training,” in *Proceedings of the IEEE/CVF Conference on Computer Vision and Pattern Recognition (CVPR)*, June 2024, pp. 15963–15974.
- [6] Fartash Faghri, Pavan Kumar Anasosalu Vasu, Cem Koc, Vaishaal Shankar, Alexander T Toshev, Oncel Tuzel, and Hadi Pouransari, “MobileCLIP2: Improving multi-modal reinforced training,” *Transactions on Machine Learning Research*, 2025, Featured Certification.
- [7] Yanghao Li, Haoqi Fan, Ronghang Hu, Christoph Feichtenhofer, and Kaiming He, “Scaling language-image pre-training via masking,” 2023.
- [8] Zineng Tang, Long Lian, Seun Eisaep, XuDong Wang, Roei Herzig, Adam Yala, Alane Suhr, Trevor Darrell, and David M. Chan, “Tulip: Towards unified language-image pretraining,” 2025, Preprint.
- [9] Alexey Dosovitskiy, Lucas Beyer, Alexander Kolesnikov, Dirk Weissenborn, Xiaohua Zhai, Thomas Unterthiner, Mostafa Dehghani, Matthias Minderer, Georg Heigold, Sylvain Gelly, Jakob Uszkoreit, and Neil Houlsby, “An image is worth 16x16 words: Transformers for image recognition at scale,” 2021.
- [10] Surat Teerapittayanon, Bradley McDanel, and H. T. Kung, “Branchynet: Fast inference via early exiting from deep neural networks,” in *Proceedings of the International Conference on Pattern Recognition (ICPR)*, 2016, pp. 2464–2469.
- [11] Yigitcan Kaya, Sanghyun Hong, and Tudor Dumitras, “Shallow-deep networks: Understanding and mitigating network overthinking,” in *Proceedings of the 36th International Conference on Machine Learning (ICML)*, Jun 2019, vol. 97 of *Proceedings of Machine Learning Research*, pp. 3301–3310, PMLR.
- [12] Stéphane G. Mallat, “A theory for multiresolution signal decomposition: The wavelet representation,” *IEEE Transactions on Pattern Analysis and Machine Intelligence*, vol. 11, no. 7, pp. 674–693, 1989.
- [13] Ingrid Daubechies, *Ten Lectures on Wavelets*, Number 61 in CBMS-NSF Regional Conference Series in Applied Mathematics. Society for Industrial and Applied Mathematics, Philadelphia, PA, 1992.
- [14] Zhenhai Zhu and Radu Soricut, “Wavelet-based image tokenizer for vision transformers,” *arXiv preprint*, 2024.
- [15] Moshe Kimhi, Shai Kimhi, Evgenii Zheltonozhskii, Or Litany, and Chaim Baskin, “Semi-supervised semantic segmentation via marginal contextual information,” 2024.
- [16] Moshe Kimhi, David Vainshtein, Chaim Baskin, and Dotan Di Castro, “Robot instance segmentation with few annotations for grasping,” in *2025 IEEE/CVF Winter Conference on Applications of Computer Vision (WACV)*, 2025, pp. 7939–7949.